

EXPERIMENTAL MODELING OF DUNE BED FORM IN A SAND-BED CHANNEL*

N. TALEBBEYDOKHTI^{1, **}, A. A. HEKMATZADEH², AND G. R. RAKHSHANDEHROO³

^{1,3}Dept. of Civil Engineering, Shiraz University, Shiraz, I. R. of Iran,
Emails: taleb@shirazu.ac.ir

²Dept. of Civil Engineering, Azad University, Eghlid, I. R. of Iran

Abstract– Resistance to flow is an important and primary parameter in the determination of water surface elevation. A variety of bed forms, especially dunes, have a sensible effect on total roughness. Because of the complexity of bed form development, previous methods differ drastically from each other in predicting dune bed forms. In this paper, laboratory experiments were conducted to investigate the geometry of dunes in a sand-bed channel and its influence on total channel resistance. The experiments were performed in a flume in the hydraulic laboratory of Shiraz University using sand particles. Simple relations were sought for dune dimensions via some dimensional parameters, and previous methods were compared to each other in light of this new data.

Keywords– Dune bed form, form roughness, dune geometry, sand-bed channel

1. INTRODUCTION

Water surface elevation is vital in the determination of flood plains boundaries and in the design of important river structures such as flood control structures, diversion dams, power plant projects, and bridges. This elevation is closely related to the resistance of erodible fluvial beds against water flow. The mutual interaction between the flow and the erodible bed through sediment transport phenomena in a sand-bed channel causes a variety of bed forms, starting with ripples, and gradually increase shear stress or water velocity, dunes, washed out dunes, flat bed, anti-dunes, and standing waves.

Total bed resistance is attributable to two roughnesses: 1) grain roughness, which in turn depends on bed grain size, and 2) form roughness, which depends on the bed form dimensions and flow depth. It is known that up to ninety percent of total channel resistance may be due to form resistance, hence this effect should not be neglected [1]. Therefore, one may conclude that it is necessary to predict accurate bed form dimensions. Furthermore, accurate prediction of bed form dimensions is important for avoiding potential problems in navigation and water diversion works. Knowing bed form geometry also enables one to estimate bed-load sediment from the continuity equation of bed particles [2].

Several investigators have done noteworthy work on dune geometry and its resistance to flow (Fig. 1). Early important works on dune geometry were done by Yalin [3], Fredsoe [reported in Raudkivi A.J. [4]], Ranja Raju and Soni [5] and Allen [6] who developed relations for dune height as a function of bed shear stress and other variables according to experimental and field data. Van Rijn [7] analyzed data from

*Received by the editors November 10, 2003; final revised form October 22, 2005.

**Corresponding author

several numbers of flumes and some field data and developed a relation for relative dune height and length as a function of flow depth, particle diameter and a transport stage parameter (function of grain and critical shear stress). Kennedy and Odgaard [8] used the concept of energy loss across a sudden expansion and derived a formula for relative dune height as a function of grain and total Darcy-Weisbach friction factor. Julien and Klaassen [9] used data of large rivers and claimed that relative dune height is independent of transport stage parameter and is only a function of relative particle diameter. Karim [10] developed relative dune height as a polynomial function of u_* / ω (ratio of shear velocity to falling velocity of particles). Karim [11] continued the study of Kennedy and Odgaard [8] and expanded this study to all bed form shapes and developed relative bed form height as a function of the energy slope gradient, relative particle diameter, Froude number and relative bed form wavelength.

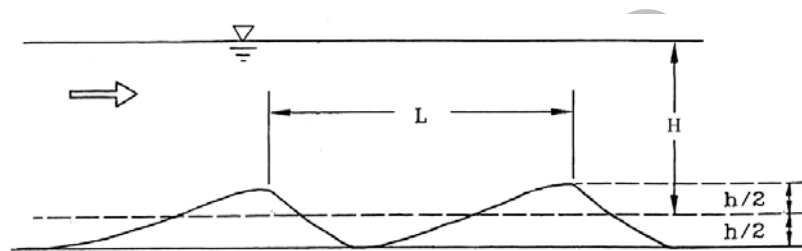


Fig. 1. Schematic view of dune

Almost all researchers estimated a value of about 4 to 7 for relative dune length. Yalin (1964), Van Rijn, Yalin [reported in Karim (1999)], Julien and Klaassen, Karim are some of them [3, 7, 11, 9].

Van Rijn [12] expressed form resistance as equivalent sand diameter and derived an exponential relation for it based on dune height and flow depth. Bruschin [reported in Raudkivi A.J. 1998] stated Manning coefficient as a function of sediment diameter, hydraulic radius and energy slope. Karim and Kennedy [13] derived friction factor ratio f / f_0 , as a function of relative dune height. Karim [10] applied regression and dimensional analysis and computed the Manning coefficient as a power function of D_{50} and f / f_0 . The results of previous investigators are briefly presented in appendix I.

Previous researchers used different approaches to find bed form dimensions. Their results differ drastically from each other and from field observations. The difference between laboratory and field conditions, lack of a reliable method for the prediction of bed form dimensions, the 3D nature of the bed form development, practical difficulties in measuring bed form dimensions, especially in fields, the role of suspended sediment in bed form creation, and the lack of knowledge about turbulence at the interface between flow and bed are among the reasons of difference in results. So the complexity of this problem indicates the need for additional research.

Experimental and numerical methods are common approaches used by researchers to model bed form formation. However, it seems that experimental approaches have more advantages than numerical approaches due to the following reasons:

- Numerical methods cannot model bed form development from a flat bed, and it is necessary that they assume an initial bed form shape. [14]
- One may use Navier-Stokes equations for turbulent flow by considering that the velocity term (u) equals mean velocity over time (\bar{u}), plus turbulence intensities (u'). In alluvial beds, however, the turbulence structure depends on the bed-form shape. For example, the turbulence on a ripple is deduced from ejection and the sweep of sediments by flow at their interface, while on dune turbulence it is produced from bursting phenomena and vertical vortex. In this case, experimental results may be considered more reliable because this type of turbulence has not yet been completely discovered, and there is an uncertainty in using u' [15].

- In some conditions, turbulent flow in alluvial beds have a coherent structure and therefore large scale eddies may develop in the flow and convert to vertical vortices called Kolk-Boils. These vortices can suspend many particles, while almost all common numerical methods use the bed-load continuity equation as the governing equation, ignoring such suspensions of particles.

It is necessary to note that among bed form features, the most common is that which takes place in sand-bed rivers are dunes. Moreover, dunes have the largest dimensions and, consequently, have the greatest and resistance to flow compared to the others.

In this paper, laboratory experiments were conducted to investigate the geometry of dunes in a sand-bed channel and its influence on total channel resistance. The experiments were performed in a flume in the hydraulic laboratory of Shiraz University using sand particles. Simple relations were sought for dune dimensions via some dimensional parameters and previous methods were compared to each other in light of this new data.

2. EXPERIMENTAL SETUP

It is known that sediment and flow variables like flow depth, flow velocity, water surface gradient, sediment diameter and its distribution and type, are the main parameters influencing the bed forms [16]. In this paper, a one-dimensional experimental model was employed to simulate bed form generation under different sediment and flow conditions. A 30 m long, 1 m wide, and 0.75 m tall rectangular concrete flume located in the hydraulic laboratory of Shiraz University, Shiraz, was utilized as shown in Fig. 1. This model consisted of a 5.5 m long and 0.5 m wide test section with two transitions at the beginning and at the end of the test section for streamlining water flow. It also included two wave suppressors for pacifying water surface, a sediment trap pool (4 m long and 1 m wide) for preventing sediments from entering the re-circulating pump system, a shutter at the end of the sediment trap pool for controlling water depth, and a sediment screen at the end of the flume for trapping extra sediment. The test section bed was elevated 0.25 m to make sufficient height for settlement of particles along the sediment trap length (4 m).

Sediment particles used in the experiments were natural quartz sand with a specific gravity of 2.65, and were sieved among four sizes (0.3, 0.5, 0.75 and 1.25mm) so that three uniform sizes of sand with average diameters of 0.4, 0.675, and 1 mm were obtained. The water flow was supplied by a pump with a maximum discharge of 80 L/sec, which was re-circulated between the upstream and downstream tanks (Fig. 2).

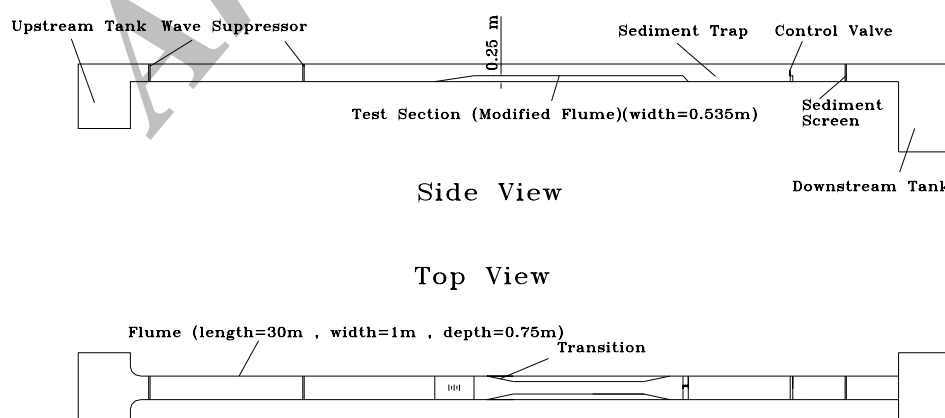


Fig. 2. Schematic view of laboratory model

At the beginning of each experiment, sediment particles were saturated to provide real natural conditions and prevent incipient motion of dry particles. They were then placed on the bed of the test section. Then, sediments were distributed and smoothed by a T-shaped device without any compaction to obtain 10 cm of sediment in height on the bed.

In these experiments, three variables were considered: 1- water depth controlled by different shutter heights and measured by a point gage. 2- Discharge rate controlled by a valve in the discharge pipe of the pump and measured by a differential orifice device. 3- Bed sand sizes (0.4 mm, 0.675 mm and 1 mm). Sand wavelets were generated within a few minutes (for example around four minutes according to Coleman [17]). Dune height was measured 15 to 30 minutes after commencement of the run. By changing the flow depth and discharge, different average velocities and Froude numbers could be obtained. The water depth and discharge rate were set in a manner so that dunes formed on the bed [10, 11]. In these experiments, the difficulty lay in measuring water surface gradient S_w . Because the water surface had fluctuations over the space and time due to bed form shapes, we had to compute S_w from existing relations. Experimental data are presented in Table 2. Figures 3 and 4 show two dune shapes of these experiments.



Fig. 3. Dune shape of run 9



Fig. 4. Dune shape of run 18

3. DERIVATION OF DUNE GEOMETRY FORMULA

a) Relative dune height ($\frac{h}{H}$)

The main parameters affecting bed form creation and development consist of the Sediment diameter, D_{50} , Sediment distribution, σ , Sediment shape, S_p , Sediment density, ρ_s , Flow depth, H , Flow velocity, V , Water density, ρ_w , Water viscosity (which includes water temperature), μ , Energy slope gradient, S_w , Earth acceleration, g , and Time, t

In this study, each test continued until equilibrium conditions were achieved. Therefore, time was eliminated from the dimensional analysis. Using the "Buckingham pi" theory for dimensional analysis, a function of the variables may be presented as:

$$h = f_1(D_{50}, H, V, \rho_w, \rho_s - \rho_w, g, S_w, \mu, S_p, \sigma) \quad (1)$$

Then, the above function may be made dimensionless as

$$\frac{h}{H} = f_2(F_r, \frac{D_{50}}{H}, \frac{\nu}{VH}, S_w, G_s - 1, S_p, \sigma) \quad \text{Where} \quad G_s = \frac{\rho_s}{\rho_w} \quad (2)$$

We can consider the power law equation between the variables of Eq. (2). In the present investigation, the three parameters $G_s - 1, S_p, \sigma$ were constant because the sediment type didn't change during the experiments and the sediment particles were uniform. So they may be included in the constant coefficient of the power law equation, and therefore eliminated from the apparent shape of the equation. Getting logarithm from the power law equation and performing the linear regression in Microsoft Excel, Eq. (3) was obtained according to the experimental data. It is necessary to say that the parameter ν / VH (reciprocal of Reynolds number) was ignored because its variables were either held constant or accounted for in other parameters.

$$\frac{h}{H} = e^{3.235} \left(\frac{D_{50}}{H} \right)^{-0.4381} (F_r)^{-2.9012} (S_w)^{1.754} \quad (3)$$

As shown in Fig. 5, a good agreement was found between measured values of h/H and the predicted value by Eq. (3). The Mean Normalized Error (MNE), (Eq. (4)) was calculated as 9.1%, which according to previous researchers is in a suitable range [10].

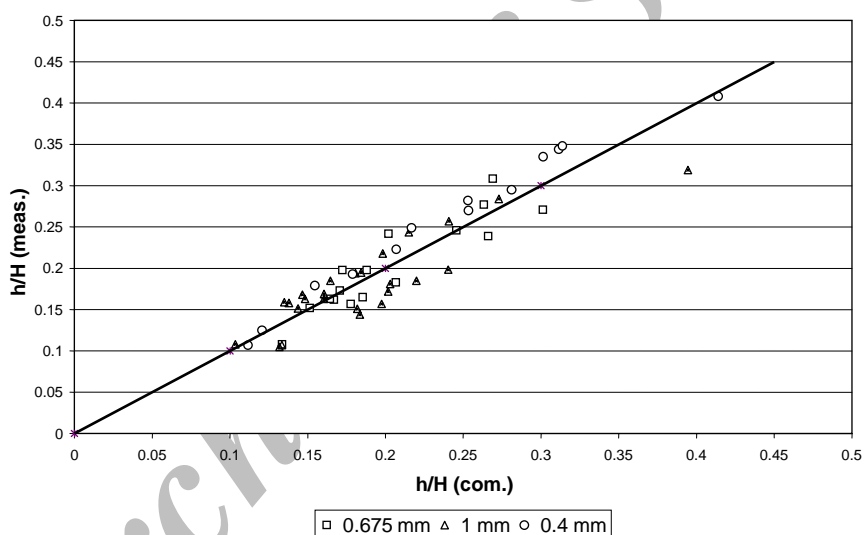


Fig. 5. Comparison diagram between measured and estimated value of h/H according to Eq. (3)

$$MNE = \frac{100}{N} \sum_{i=1}^N \frac{|x_{ci} - x_{mi}|}{x_{mi}} \quad (4)$$

Where x_{ci} and x_{mi} are the computed and measured value of h/H for the i th event, respectively and N is the number of data points. In Eq. (3), the values of h/H , D_{50}/H and F_r were computed directly from laboratory measurements, while S_w could be calculated from existing formulas such as:

- Bruschin (1985) and Manning equation, [4].
- Van Rijn and Chezy equation [7].
- Karim and Manning equation [10].

The formula of Karim was utilized because of the widespread use of the Manning equation among engineering professionals [10].

In order to investigate the effect of each parameter in Eq. (3), a sensitivity analysis was performed. Figures 6 to 8 show variations in the measured values of h/H with respect to F_r , D_{50}/H and S_w ,

respectively. As seen, it is almost impossible to make a suitable relation between h/H and each one of the above parameters alone. Therefore, it was concluded that relative dune height depends on a combination of all parameters as can be deduced from Fig. 5.

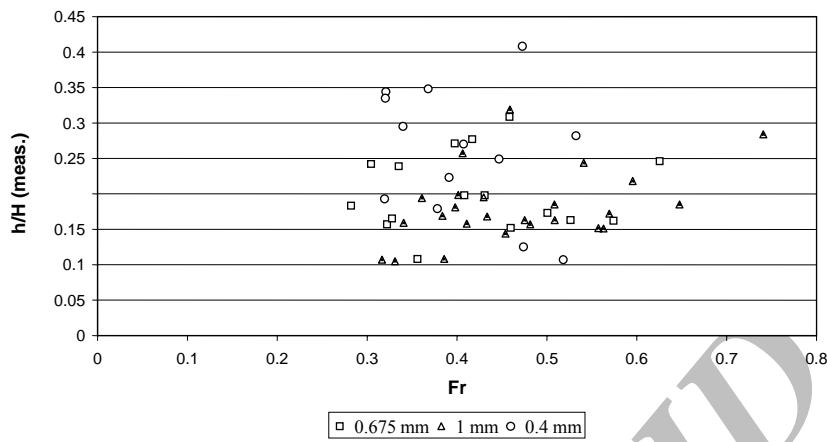


Fig. 6. Diagram of changes of h/H with respect to Fr

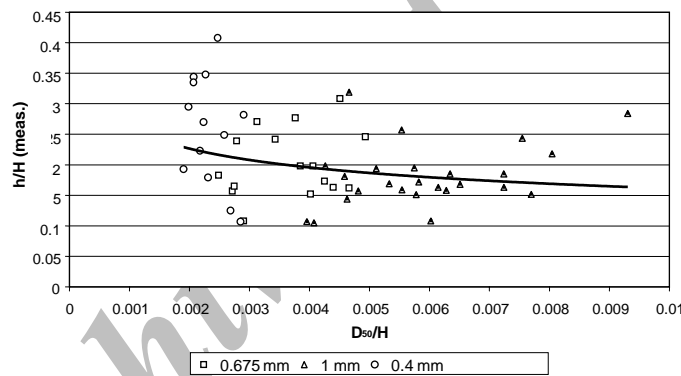


Fig. 7. Diagram of changes of h/H with respect to D_{50}/H

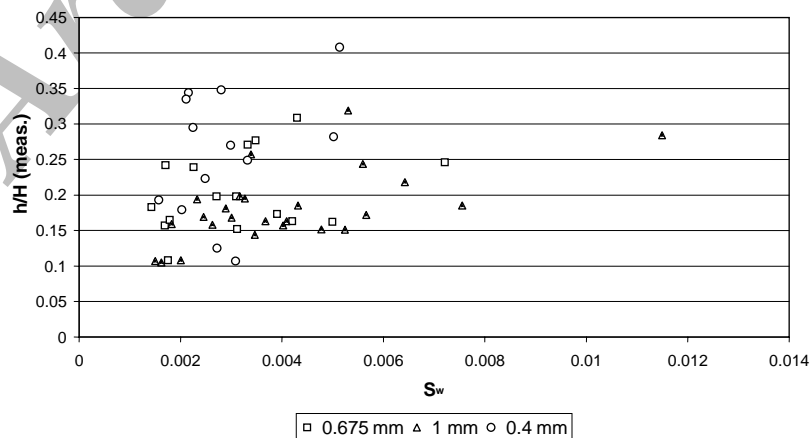


Fig. 8. Diagram of changes of h/H with respect to Sw

Because of the difficulty in estimating S_w , some researchers like Van Rijn have tried to eliminate S_w from their relations [7]. Equation (5) was obtained by a procedure similar to Eq. (3) between h/H as the

dependent variable and D_{50} / H and F_r as independent variables. By this procedure S_w was not considered as an independent variable.

$$\frac{h}{H} = 0.041 \left(\frac{D_{50}}{H} \right)^{-0.3516} (F_r)^{0.4466} \quad (5)$$

As shown in Fig. 9, good agreement was not found between measured values of h/H and the predicted values obtained by Eq. (5). So it was concluded that the effect of S_w is sensible.

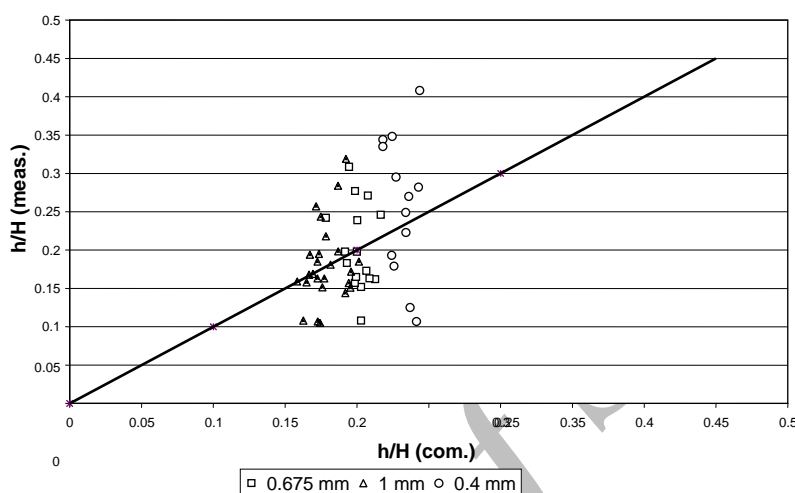


Fig. 9. Comparison diagram between measured and estimated value of h/H according to Eq. (5). Good agreement wasn't found between measured values of h/H and the predicted values

b) Relative dune length ($\frac{L}{H}$)

Relative wavelength ratios L/H have usually been found to be in the range of 4 to 7 [16]. In this study, this ratio was obtained about 4.5 as can be seen in Fig. 10 and Eq. (6). An attempt was made to construct a relation similar to Eq. (3) between L/H as a dependent variable and S_w , D_{50} / H and F_r as independent variables. So, Eq. (7) was obtained, but offered no better prediction than Eq. (6) according to the Mean Normalized Errors and Figs. 10 and 11.

$$L/H = 4.5 \quad \text{MNE} = 21.9 \% \quad (6)$$

$$L/H = 22.81 (Fr)^{0.0366} (D_{50} / H)^{0.1284} (S_w)^{0.14986} \quad \text{MNE} = 19.8 \% \quad (7)$$

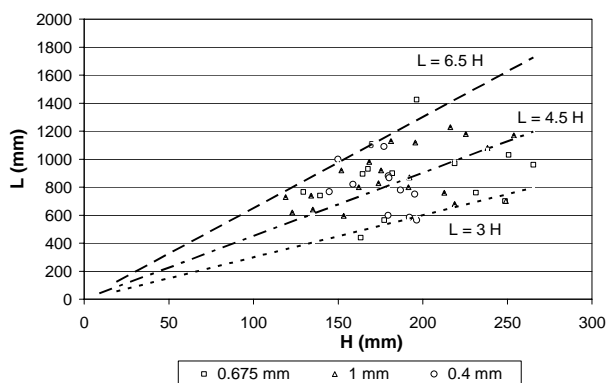


Fig. 10. Diagram of changes of L (sand wave length) with respect to H (water depth)

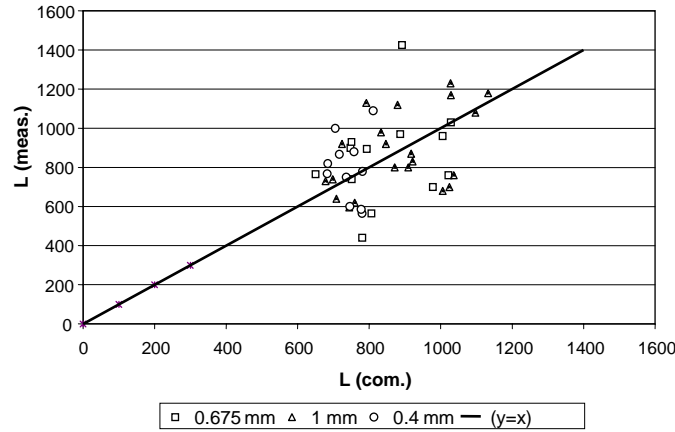


Fig. 11. Comparison diagram between measured and estimated value of L according to Eq. (7)

c) Form roughness effect

The Manning equation has been used widely by most hydraulic engineers for different purposes. We used the Manning coefficient, n , as a base for comparison between form roughness (n'') and total roughness (n). Figures 12 and 13 show variation in n''/n and n with respect to the measured value of h/H where n'' has been estimated by Eq. (8).

$$n'' = n - n' \tag{8}$$

In the above equation, n was computed by the Manning equation (velocity and hydraulic radius were obtained from the measured value, and S_w was computed as described before), and n' (grain roughness was estimated from Strickler's relation, (1923) which is suitable for sand particle [2] written as Eq. (9)

$$n = \frac{D^{1/6}}{21.1} \text{ In SI unit} \tag{9}$$

Figure 12 shows that 25-50 percent of n consist of n'' . It is obvious that a 50 percent increase in the Manning coefficient makes a 66 percent increase in water depth in a wide channel, so this effect is not negligible.

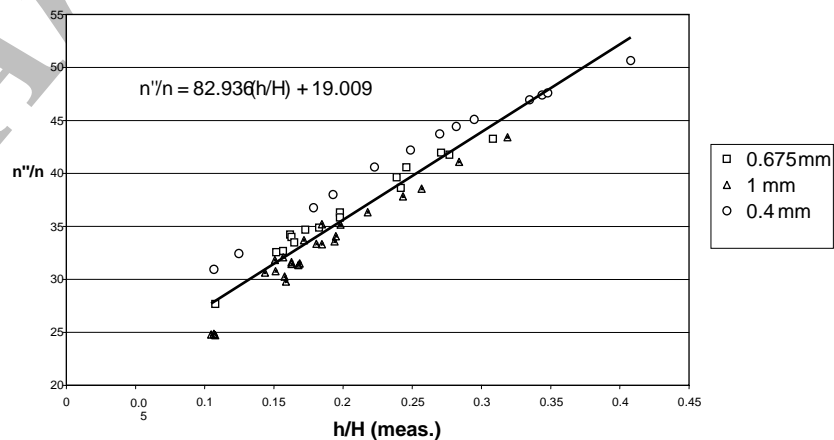


Fig. 12. Diagram of changes of n''/n with respect to h/H

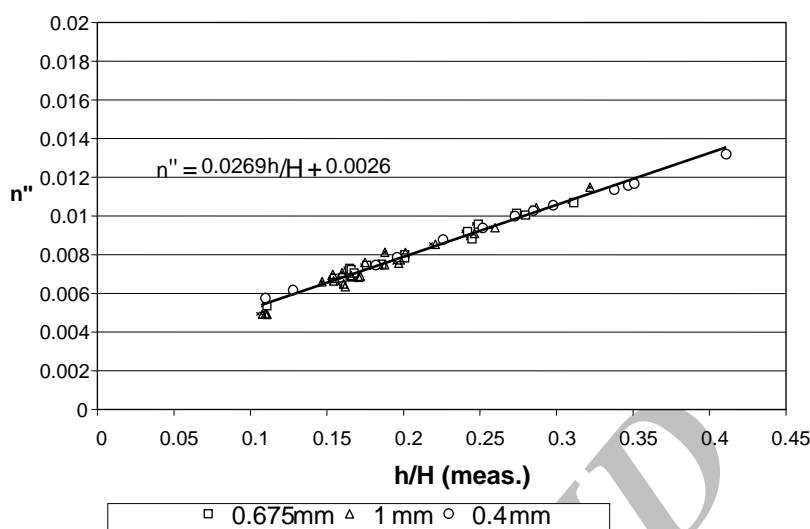


Fig. 13. Diagram of changes of n'' with respect to h/H

Based on data from our study, the form roughness $\frac{n''}{n}$, n'' was found based on linear regression as Eqs. (10) and (11). Figures 12 and 13 show these relations.

$$\frac{n''}{n} = 82.938 \left(\frac{h}{H} \right) + 19.01 \quad (10)$$

$$n'' = 0.0269 \left(\frac{h}{H} \right) + 0.0026 \quad (11)$$

4. COMPARISON

According to these laboratory data, the previous methods compare with each other. The MNE of these methods are presented in Table 1. Also, Figs. 14 and 15 show the measured and computed value of h/H . Based on the above table and figure, Yalin's method [3] predicted 0.15 to 0.16 for values of h/H for all flow conditions, while measured values of h/H were in the range of 0.1 to 0.4. Ranja Raju and Sonis' formula [5] underestimated the values of h/H a little. But with respect to the other methods, its accuracy was satisfactory. Karim's method [10] underestimated values of h/H more than Ranja Raju and Sonis' method, but its accuracy was accessible. Julien and Klaassens' relation [9] yields the worst results and greater overestimated values of h/H because this method was based on data from large rivers. Karim's method [11] many times overestimated the value of h/H , making it unsatisfactory. This method is sensitive to values of L/H . It seems that the methods of Van Rijn [7] and Kennedy and Odgaard [8] have an average accuracy with respect to the others, but these methods overestimate the values of h/H . Fredsoe's method (reported in [4]) is extremely sensitive to L/H . If $L/H = 4.5$ then $MNE=29.3\%$ with a maximum of 0.25 for the predicted values of h/H , and if $L/H = 6.25$, then $MNE=63.9\%$ with a maximum prediction of 0.35. So this method is not reliable.

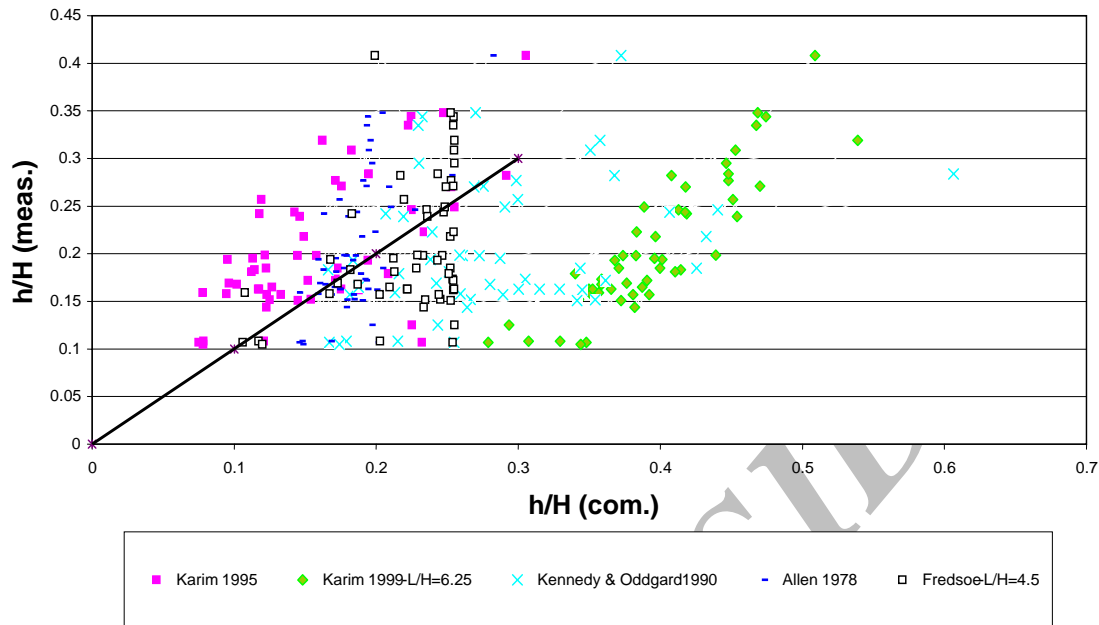


Fig. 14. Comparison diagram between measured and estimated value of h/H according to existing methods

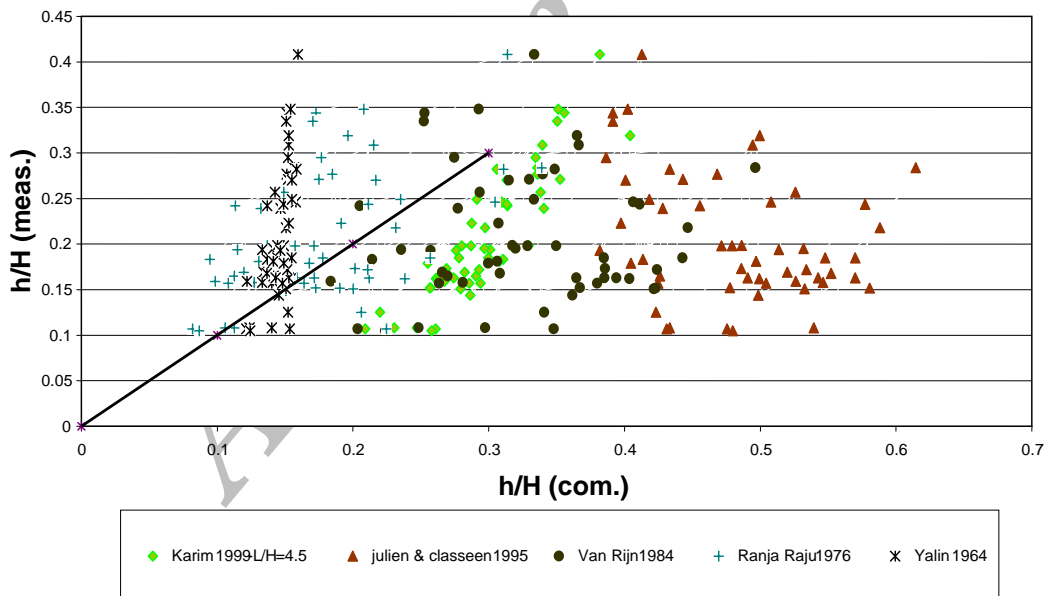


Fig. 15. Comparison diagram between measured and estimated value of h/H according to existing methods

5. CONCLUSION

- The effect of form resistance is not negligible ($n''=0.25-0.55 n$).
- The combination of dimensional and regression analysis give satisfactory results in the derivation of an appropriate formula for h/H ratio.

- Equation (10) gives us a simple relation for computing the form roughness (due to dune), which is useful in the trial and error process.
- h/H Ratio is dependent on the combination of three parameters S_w , D_{50}/H and F_r . If one of the dimensionless parameters is eliminated, error would increase.
- It seems that the constant value of 4.5 for the L/H ratio has sufficient accuracy with respect to complex formula.
- Existing methods give different approximations for the prediction of dune dimensions.
- Methods of Ranga Raju and Soni [5] and Karim [10] give better prediction for relative dune height compared to previous methods.

NOMENCLATURE

D_{50}	Mean Sediment diameter
H	Flow depth
L	Dune length
V	Flow velocity
F_r	Froude Number
S_w	Energy slope gradient
S_p	Sediment shape factor
h	Dune height
g	Gravitational acceleration
t	Time
u_*	Shear velocity
f	Darcy-Weisbach friction factor (including contribution due to bed forms)
f_0	Darcy-Weisbach friction factor due to grain roughness only

Greek Symbols

ρ_s	Sediment density,
ρ_w	Water density
μ	Water viscosity
σ	Sediment size distribution factor
w	Falling velocity of sediment particles

REFERENCES

1. Kazemipour, A. K. & Apelt, C. J. (1983). Effects of irregularity of form on energy losses in open channel flow. *Australian Civil Eng. Transactions, I.E. Aust., CE25*, 294-299.
2. Yang, C. T. (1996). *Sediment transport: theory and practice*. Mc Grow-Hill Ltd.
3. Yalin, M. S. (1964). Geometrical properties of sand waves. *J. Hydr. Dir., ASCE, Val 90(5)*, 105-119.
4. Raudkivi, A. J. (1998). *Loose boundary hydraulics*. Rotterdam, Balkema A.A. Ltd.
5. Ranga-Raju, K. G. & Soni, J. P. (1976). Geometry of ripples and dunes in alluvial channels. *J. Hydr. Res., Oelft, the Netherlands, 14 (3)*, 241-249.
6. Allen, J. R. L. (1978). Computational methods for dune time-lag: calculations using stein's rule for dune height. *Sedimentary Geology, 20(3)*, 165-216.
7. Van-Rijin, L. C. (1984). Sediment transport, Part III: Bed forms and alluvial roughness. *J. Hydr. Eng., ASCE, 110 (12)*, 1733-1753.

8. Kennedy, J. F. & Odgaard, A. J. (1990). *An informal monograph on riverine sand dunes*. IIHR Ltd. Distribution Rep. No. 169, Iowa Inst. Of Hydr. Res., University of Iowa, Iowa.
9. Julien, P. Y. & Klaassen, G. J. (1995). Sand–Dune geometry of large rivers during floods. *J. Hydr. Eng., ASCE*, 121 (9), 657–663.
10. Karim, M. F. (1995). Bed configuration and hydraulic resistance in alluvial–channel flows. *J. Hydr. Eng., ASCE*, 121(1), 15–25.
11. Karim, F. (1999). Bed–form geometry in sand bed flows. *J. Hydr. Eng., ASCE*, 125(12), 1253–1261.
12. Van–Rijin, L. C. (1982). Equivalent roughness of alluvial bed. *J. Hydr. Div., ASCE*, 108(10).
13. Karim, M. F. & Kennedy, J. F. (1990). Menu of coupled velocity and sediment discharge relations for rivers. *J. Hydr. Eng., ASCE*, 116(8), 978–996.
14. Coleman, S. E. & Melville, B. W. (1994). Bed–form development. *J. Hydr. Eng., ASCE*, 120(4), 544 – 560.
15. Nezu, I. & Nakagawa, H. (1992). *Turbulence in open channel flows*. IAHR, Rotterdam, Balkema A.A. Ltd.
16. Carling, P. A. & Dawson, M. R. (1996). *Advanced in fluid dynamics and stratigraphy*. John Wiley & Sons ltd. Chapter 3.
17. Coleman, S. E. & Melville, B. W. (1996). Initiation of bed forms on a flat sand bed. *J. Hydr. Eng., ASCE*, 122(6), 301 – 310.

APPENDIX

I (Existing relations for dune geometry and its resistance to flow):

Yalin (1964):

$$\frac{h}{H} = \frac{1}{6} \left(1 - \frac{\tau_{cr}}{\tau_o} \right) \text{ and } L = 5H \text{ where } \tau_{cr} = \text{critical shear stress for } D_{50}; \text{ and } \tau = \text{bed shear stress}$$

Yalin (1972):

$$L = 2\pi$$

Fredsoe (1975):

$$\frac{h}{H} = 0.119 \left(\frac{L}{H} \right) \left(1 - \frac{0.06}{\theta} - 0.4\theta \right)^2 \text{ where } \theta = \text{dimensionless bed shear stress (Shields parameter)}$$

Ranga Raju & Soni (1976):

$$\frac{h}{D_{50}} F_1^3 F_2 = 6.5 \times 10^3 (\tau_*')^{\frac{8}{3}} \text{ where } F_1 = \frac{V}{\sqrt{gR_b}}; F_2 = \frac{V}{\sqrt{\frac{\gamma_s - \gamma}{\rho} D_{50}}}; \tau_*' = \text{dimensionless bed shear stress}$$

due to grain roughness

Allen (1978):

$$\frac{h}{d} = 0.08 + 2.24 \left(\frac{\theta}{3} \right) - 18.13 \left(\frac{\theta}{3} \right)^2 + 70.9 \left(\frac{\theta}{3} \right)^3 - 88.33 \left(\frac{\theta}{3} \right)^4 \text{ where } \theta = \text{dimensionless bed shear stress}$$

(Shields parameter)

Van Rijn (1982):

$$K_{s,form} = 1.1h \left(1 - e^{-25 \frac{h}{H}} \right) \text{ where } K_{s,form} = \text{equivalent sand diameter}$$

Van Rijn (1984):

$$\frac{h}{H} = 0.11 \left(\frac{D_{50}}{H} \right)^{0.3} \left(1 - e^{-0.5T} \right) (25 - T) \text{ and } L = 7.3H \text{ where } T = \frac{(u_*')^2 - (u_{*scr})^2}{(u_{*scr})^2}; T = \text{transport stage}$$

parameter; u_*' = bed shear velocity related to grains; u_{*scr} = critical bed shear velocity

Bruschin(1985):

$$n = \frac{D_{50}^{1/6} \left(\frac{RS_w}{D_{50}} \right)^{1/7.3}}{12.8} \quad \text{where } R = \text{hydraulic radius}$$

Kennedy & Odgaard (1990):

$$\frac{h}{d} = \frac{1}{2} \left\{ \frac{1.2\lambda\alpha f_0}{8C_D} + \left[\left(\frac{1.2\lambda\alpha f_0}{8C_D} \right)^2 + \frac{2\pi F^2 f_0}{C_D C_1} \left(\frac{f}{f_0} - \frac{1.2\lambda}{2} \right) \right]^{0.5} \right\} \quad \text{where } f_0, f = \text{grain and total Darcy-}$$

Weisbach friction factor; F=froude number; and $C_1 = 0.25, C_D = 1.0, \alpha = 5, \lambda = 1.0$

Karim and Kennedy (1990)

$$\frac{f}{f_0} = 1.2 + 8.92 \left(\frac{h}{H} \right)$$

Julien & Klassen (1995):

$$\frac{h}{H} = \xi \left(\frac{D_{50}}{H} \right)^{0.3} \quad \text{and } L = 6.25H \quad \text{where } 0.8 < \xi < 8 \quad \text{and } \xi_{avr} = 2.5$$

Karim (1995):

$$\frac{h}{H} = -0.04 + 0.294 \left(\frac{u_*}{\omega} \right) + 0.00316 \left(\frac{u_*}{\omega} \right)^2 - 0.0319 \left(\frac{u_*}{\omega} \right)^3 + 0.00272 \left(\frac{u_*}{\omega} \right)^4 \quad \text{where } u_* = \text{bed shear}$$

velocity; and ω = particle fall velocity for D_{50}

$$n = 0.037 D_{50}^{0.126} \left(\frac{f}{f_0} \right)^{0.465} \quad \text{where } D_{50} \text{ in meters and } n \text{ in SI units}$$

Karim (1999):

$$\frac{h}{H} = \frac{\left(S - f' \frac{F^2}{8} \right) \lambda}{KF^2 C_1} \quad \text{where } K = 0.55 \left(\frac{h}{H} \right)^{0.375} \left(\frac{\lambda}{H} \right)^{-0.2}; \quad f' = 0.135 \left(\frac{D_{50}}{H} \right)^{0.33}; \quad C_1 = 0.85;$$

$$\frac{\lambda}{H} = 6.25; \quad S = \text{energy slope gradient; and } F = \text{froude number}$$

Appendix II

Table 1. Table of MNE error of existing methods

Researcher name	MNE
Yalin (1964)	% 27.4
Ranga Raju & Soni (1976)	% 27.2
Allen (1978)	% 27.1
RijnVan (1984)	% 78.7
Julien & Klassen (1995)	% 162.1
Karim (1995)	% 28.7
Karim (1999)- L/H=6.25	% 104.9
Karim (1999)- L/H=4.5	% 53.9
Fredsoe (1975)	% 29.3
Kennedy & Odgaard (1990)	% 53.8
Our result	% 9.1

Table 2. Experimental data

1	2	3	4	5	6
H-mm	h-mm	D50-mm	V-m/s	Fr	Sw
168.0	25.5	0.675	0.590	0.460	0.003744
158.7	27.5	0.675	0.625	0.501	0.004697
144.9	23.5	0.675	0.684	0.574	0.005891
175.4	34.7	0.675	0.565	0.431	0.003809
153.5	25.0	0.675	0.646	0.526	0.005007
136.8	33.7	0.675	0.725	0.626	0.008755
179.3	49.7	0.675	0.553	0.417	0.004365
196.8	47.6	0.675	0.423	0.304	0.002185
149.7	46.2	0.675	0.556	0.459	0.005482
166.3	32.9	0.675	0.521	0.408	0.003383
271.5	49.7	0.675	0.460	0.282	0.001756
242.1	57.8	0.675	0.516	0.335	0.00278
248.5	39.0	0.675	0.503	0.322	0.002057
245.7	40.5	0.675	0.509	0.328	0.002175
216.0	58.5	0.675	0.579	0.398	0.004089
232.5	25.1	0.675	0.538	0.356	0.002074
180.6	46.4	1	0.541	0.406	0.004377
195.5	37.9	1	0.500	0.361	0.002984
187.6	31.7	1	0.521	0.384	0.003108
174.0	33.9	1	0.561	0.430	0.004141
162.7	26.5	1	0.600	0.475	0.00455
124.3	27.1	1	0.657	0.595	0.008076
107.5	30.5	1	0.761	0.741	0.014519
166.0	17.9	1	0.492	0.386	0.002488
159.2	25.2	1	0.513	0.411	0.003334
153.6	25.8	1	0.532	0.434	0.003809
180.4	28.7	1	0.453	0.341	0.002352
132.5	32.3	1	0.617	0.541	0.00716
129.9	19.7	1	0.629	0.557	0.005851
138.1	25.5	1	0.592	0.508	0.005434
138.1	22.5	1	0.592	0.509	0.005091
252.7	27.0	1	0.498	0.317	0.00185
245.3	25.8	1	0.513	0.331	0.001989
218.0	39.5	1	0.582	0.398	0.003592
173.0	26.1	1	0.733	0.563	0.006213
171.7	29.5	1	0.739	0.570	0.006782
157.6	29.2	1	0.805	0.648	0.00898
216.0	31.1	1	0.661	0.454	0.00415
207.7	32.6	1	0.687	0.481	0.004823
234.5	46.5	1	0.609	0.401	0.003918
214.5	68.4	1	0.665	0.459	0.006659
201.7	59.5	0.4	0.478	0.340	0.002718
178.8	48.3	0.4	0.539	0.407	0.003593
210.3	40.6	0.4	0.459	0.319	0.001884
183.7	41.0	0.4	0.525	0.391	0.00297
161.9	66.1	0.4	0.596	0.473	0.006244
193.2	66.4	0.4	0.442	0.321	0.002649
148.9	18.6	0.4	0.573	0.474	0.00312
154.9	38.6	0.4	0.551	0.447	0.004009
173.1	31.0	0.4	0.493	0.378	0.002428
137.8	38.9	0.4	0.619	0.532	0.006051
176.3	61.4	0.4	0.484	0.368	0.003444
140.3	15.0	0.4	0.608	0.518	0.003461
193.4	64.8	0.4	0.441	0.320	0.002595